# Atomic structure and optical properties of GeSi nanostructures obtained by implantation of $Ge^+$ ions into silicon followed by thermal annealing

© Zh.V. Smagina[1], V.A. Zinovyev[1], A.F. Zinovieva[1], V.A. Volodin[1], I.A. Aleksandrov[1], A.K. Gutakovskii[1], V.I. Vdovin[1], A.V. Mudryi[2], V.D. Zhivulko[2], V.E. Zakharov[3], L.I. Fedina[1]

[1] Rzhanov Institute of Semiconductor Physics of the Siberian Branch of the Russian Academy of Sciences, Novosibirsk, Russia
[2] Scientific-Practical Material Research Centre of the National Academy of Sciences of Belarus, Minsk, Belarus
[3] Institute for Physics of Microstructures of the Russian Academy of Sciences, Nizhny Novgorod, Russia

E-mail: smagina@isp.nsc.ru

*Received March 31, 2026*
*Revised May 28, 2026*
*Accepted May 28, 2026*

A comparative analysis of the structure and optical properties of extended defects introduced by $Ge^+$ ion implantation and subsequent annealing at $T = 500-800\,^\circ$C into silicon layers in SOI structures and Si(100) wafers was performed. In both cases, up to $600\,^\circ$C, extended {113} defects dominate in the structure of the implanted layers (with the proportion of {001} defects no more than $\sim 5\%$). However, at $T = 700\,^\circ$C, {001} defects become the main ones in Si wafers, and the geometric phase analysis of their HRTEM images reveals significant nano-fluctuations of elastic strains in the {001} plane of the defect, indicating a variation in its atomic structure and possible Ge segregation. In an SOI structure annealed at $T = 800\,^\circ$C, both types of defects disappear according to photoluminescence (PL) data, but at $T < 800\,^\circ$C, the PL spectra qualitatively reproduce the light emission features in the range of 1.2–1.6 $\mu$m in both cases. The obtained PL quenching activation energies indicate its lower thermal stability in the SOI structure compared to Si(100) wafer.

**Keywords:** ion implantation, germanium, silicon on insulator, thermal annealing, high-resolution electron microscopy, {113} and {001} defects, photoluminescence.

DOI: 10.61011/SC.2026.02.63745.9369

## 1. Introduction

One of the promising areas for the development of modern microelectronics is integral silicon-based photonics [1–4]. The main problem in designing highly efficient sources of radiation based on silicon is related to its nondirect band gap structure. Among multiple assumptions to solve this problem, an idea stands out to use Ge/Si heterostructures with quantum dots (QDs) [5–7]. Today several potential implementations of the sources of radiation based on Ge–Si-heterocouple have been proposed: (i) GeSi-quantum dots, grown epitaxially; (ii) GeSi QDs developed using low-energy ion implantation; (iii) various extended defects arising from ion implantation and annealing. The promising nature of (ii) and (iii) approaches has already been confirmed [8–15]. For epitaxial structures with ion-modified GeSi QDs, the multiple increase in photoluminescence (PL) intensity and high thermal stability of PL were obtained compared to the same structures without implantation [8–13]. Extended {113} defects and GeSi nanoinclusions with size of $\sim 10$ nm and higher Ge content (analog of „QD“) in silicon implanted with ions $Ge^+$, which arise, accordingly, after annealing at 700 and $800\,^\circ$C, also demonstrate stable PL up to room temperatures in the region of $1.3-1.6\,\mu$m [14]. In this paper, using the analysis of the geometric phase of images (produced by high resolution electron microscopy (HREM) of the {113} defects, we have demonstrated that the PL stabilization with the use of ion implantation of Ge into Si may be based on nanosegregation of Ge atoms, both in the plane of defects and in the form of nano-QDs, which may provide for direct intraband optical transitions and, accordingly, high efficiency of radiative recombination. When GeSi QDs are used with defects, the effect of laser generation was demonstrated as the optically active medium built into the silicon disc microresonant cavity [9]. For the GeSi-nanostructures obtained using regular ion implantation of germanium into silicon and subsequent thermal annealing, such experiment is a relevant task. To solve it, it is necessary to build the GeSi-nanostructures with the optically active defects into microresonant cavities. The most promising from the point of view of scaling and introduction into the modern technological cycles are the resonant cavities developed on the silicon-on-insulator (SOI) substrates with the help of lithography and subsequent plasma chemical etching through a mask. To move towards this technology, at the first step it is necessary to check how the type of the substrate affects the process of formation of the defects and their luminescent properties. Therefore, the objective of this paper is to conduct the comparative analysis of the structure and optical properties of extended defects arising in the SOI structures and reference plates Si(001) with $Ge^+$ ion implantation and subsequent thermal annealing.

## 2. Methods and details of the experiment

Light-emitting structures were created using $Ge^+$ ion implantation into silicon and subsequent thermal annealing in the wide range of temperatures $T = 300-800\,^\circ C$ (with the pitch of $100\,^\circ C$) in the nitrogen atmosphere for 20 min. The conditions of implantation were selected on the basis of our previous studies [14]. For the experiments, we used p-type Si (001) wafers and SOI substrates with the upper Si $\sim 240$ nm layer and buried $SiO_2$ $\sim 3\,\mu m$ layer. Since the buried layer of oxide helps to dissolve the extended defects [16], in order to reduce this effect, an additional layer of silicon was grown with thickness of 260 nm on the SOI substrate. As a result, the total thickness of the upper silicon layer was $\sim 500$ nm, which is the optimal parameter for the formation of microresonant cavities [17]. Si growth was carried out in a unit of molecular beam epitaxy SIVA-21 by Riber with gradual increase of temperature from 500 to $600\,^\circ C$. Implantation of $Ge^+$ ions with energy of 80 keV, dose of $10^{15}\,cm^{-2}$ and current density of $\sim 2\,\mu A/cm^2$ was carried out at room temperature on an ion beam accelerator IBA-3 (Kazan Physical-Technical Institute, Federal Research Center, Kazan Scientific Center, Russian Academy of Sciences).

The crystalline structure and elemental composition in the obtained structures were studied by Raman scattering (RS) spectroscopy method. A spectrometer T64000 (Horiba Jobin Yvon, France) was used, the spectral resolution was not inferior to $2\,cm^{-1}$. Raman scattering (RS) spectra were recorded in the back-scattering geometry, the source of excitation was argon laser with wavelength of 514.5 nm using a micro-Raman attachment. The diameter of the analyzing beam of light was $\sim 10\,\mu m$, the power of light incident on the sample was $\sim 1$ mW.

The atomic structure of the samples made in the (110) cross section was studied with the help of high resolution electron microscopy using microscope Titan 80-300 with electron energy of 200 keV and correction of spherical aberration. The maps of elastic stress distribution in the plane of extended defects were obtained from the geometric phase analysis (GPA) of their HRTEM images.

The studies of luminescent properties of GeSi-nanostructures were conducted using a solid state laser with wavelength of 405 nm in the wide temperature range of 5.3–300 K. Photoluminescence spectra were recorded on a monochromator MDR-23U using a nitrogen-cooled Ge-detector of EO-817H type.

## 3. Experiment results and discussion

Figure 1 presents the RS spectra of SOI structures after implantation of $Ge^+$ ions and annealing in a wide temperature range of $300-800\,^\circ C$. Under the conditions of

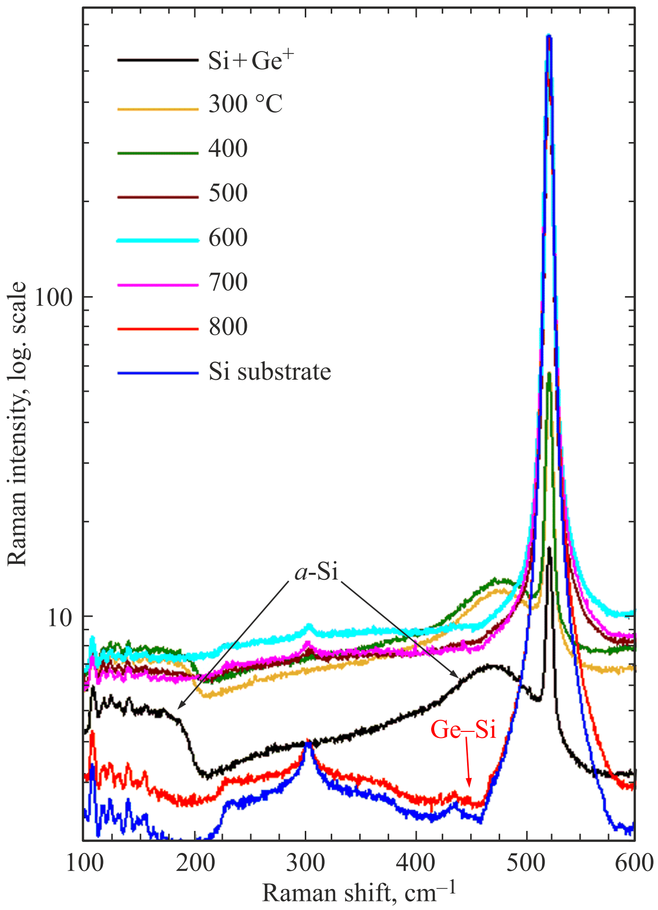


**Figure 1.** RS spectra for SOI structures after implantation of $Ge^+$ ions and subsequent annealing in the temperature interval of $300-800\,^\circ C$.

implantation that we selected, silicon partially amorphizes, which is indicated by the features in the RS spectra observed in the frequency range $150-200\,cm^{-1}$ and $450-500\,cm^{-1}$ (Figure 1, black curve). Increase of annealing temperature causes silicon recrystallization, so that after anneaing at $T = 800\,^\circ C$ the spectrum will not differ from the spectrum of single-crystal silicon (Figure 1, red curve). However, in this spectrum a very weak feature is observed at the frequency of vibrations $447\,cm^{-1}$, which may be related to the local vibrations of germanium in the silicon matrix, possibly related to Ge segregation in the plane of extended {001} defects, as we will demonstrate further. The spectra also include features related to two-phonon scattering in acoustic phonons in the silicon substrate. Figure 1 shows the spectrum of the silicon substrate, for convenience the intensity of RS spectra is shown at logarithmic scale.

Analysis of atomic structure of SOI samples annealed at $600\,^\circ C$ demonstrated that the main extended defects in the implanted layers of silicon were {113} defects. Their HRTEM images are presented in Figure 2, *a* and *b* for different depth of occurrence of {113} defects from the surface: in the field of projected path ($R_p$) of ions $Ge^+$

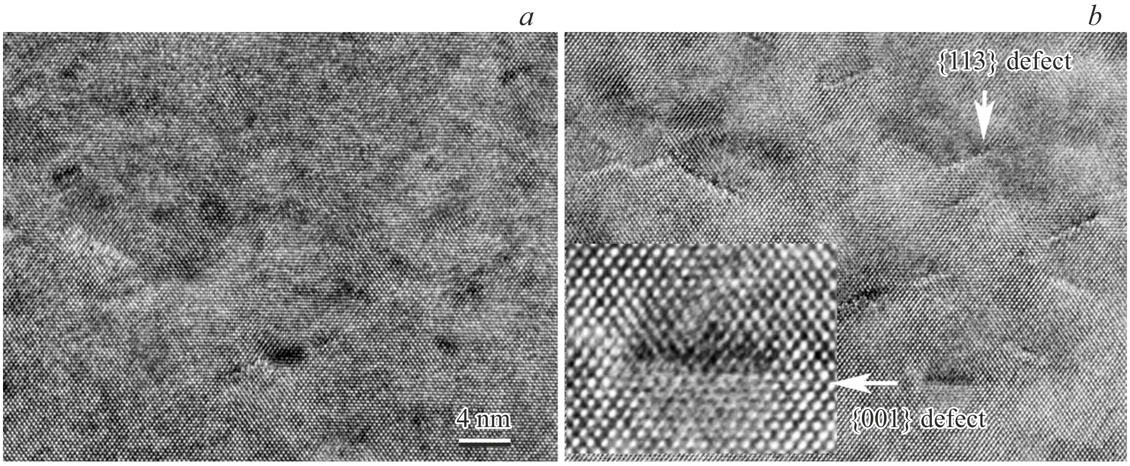


**Figure 2.** HREM images of extended defects in a SOI structure implanted by $Ge^{+}$ ions with energy of 80 keV and annealed at $T = 600\,^{\circ}C$: *a* — image obtained at depth of 60−70 nm from the sample surface; *b* — image obtained at depth of > 70 nm.

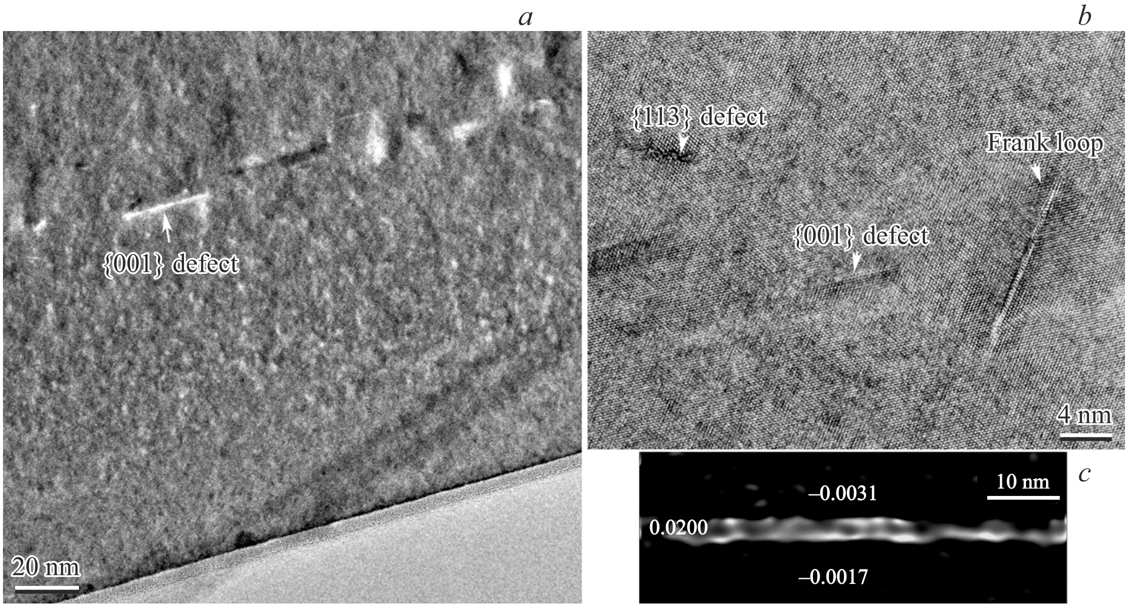


**Figure 3.** HREM images of extended defects in Si(001) implanted with $Ge^{+}$ ions, after annealing at $T = 700\,^{\circ}C$ with low (*a*) and high magnification (*b*). *c* — map of stress distribution in the plane of a large {001} defect marked with an arrow on a panel *a*. The averaged positive value of deformations inside the defect corresponds to its vertical (Eyy) tension of $\sim 2$ %, and the negative ones beyond the defect — to weak compression. Small spots with the maximum intensity correspond to 4 % deformation related to the Ge segregation in the plane of the defect.

($\sim 60$ nm [18,19]) and at the depth of slightly more than 70 nm, accordingly. In the area $R_p$ the transverse size of {113} defects is 2.4 nm (Figure 2, *a*) and increases up to 5.7 nm with the growth of the depth of occurrence of defects (Figure 2, *b*). You can also see that a HREM image in the plane of defects varies strongly from a defect to a defect, so that their structure may not be defind unambiguously. Apart from {113} defects in the implanted layer annealed at $T = 600\,^{\circ}C$, there is a small proportion ($\leq 5$ %) of {001} defects (see insert in Figure 2, *b*), the HREM image of which is related to the increase in the contrast and slight extension of atomic columns (dark spots) in the plane of the defect. As the annealing temperature increases to $T = 800\,^{\circ}C$, according to the PL data, the extended defects in the SOI structure are annealed, therefore the atomic structure of these samples using the HREM method was not studied. However, in the implanted Si(001) after annealing at $T = 700\,^{\circ}C$ there is a cardinal change of domination of {113} defects to {001} defects with the significant increase of their cross section dimensions to 40 nm (Figure 3, *a*) and appearance of Frank dislocations of the interstitial type (Figure 3, *b*). Besides, the analysis of the geometric phase of the HREM image of {001} defects shows the presence of considerable fluctuation of elastic stresses reaching 4%, which indicate the segregation of germanium (Figure 3, *c*).

As it is known, the structure of all extended metastable {113}, {001}, {111} defects arising under radiation exposure, is very complicated and depends on the mix aggregation of self-interstitial atoms and vacancies [20–22]. Under ion implantation it cannot be decoded, also due to the segregation of the implanted impurity in the plane of the defects creating strong variations of contrast on a HREM image of the defect [14]. However, at the initial stage of {113} defect formation studied in detail in Si(110) samples at *in situ* HREM radiation with electrons with energy of 400 keV, its plane clearly shows atomic columns extended ($\sim 30\%$) in direction [001], which, in accordance with the calculated HREM images, correspond to the interstitial atoms split in direction $\langle 110 \rangle$ ($I_{\langle 110 \rangle}$) [22]. Previously under radiation with electrons of Ge crystals the split Ge$-I_{\langle 110 \rangle}$ were fixed also in the plane of {001} defects [20]. It is surprising that $I_{\langle 110 \rangle}$ in the plane of {113} defects are fixed in the Si layers implanted with $Ge^{+}$ ions after annealing at $T = 700\,^{\circ}$C [14], which directly indicates their stability, possibly related to the formation of Ge$-I_{\langle 110 \rangle}$. Recent ab initio calculations of optical properties of the split Ge$-I_{\langle 110 \rangle}$ in the solid solution $Si_{0.6}Ge_{0.4}$ have already demonstrated the possibility for appearance of direct radiative transitions in the energy interval of $\sim 0.8-0.9$ eV [8]. However, despite the possibility of observation, the question on the direct relation of Ge$-I_{\langle 110 \rangle}$ and optical transition in the field of 0.8 eV requires more thorough structural studies.

Figure 4, *a* and *b* show the PL spectra of the SOI structure implanted with germanium after annealing at $T = 600$ and $700\,^{\circ}$C accordingly, which demonstrate the evolution of $G2$, $G1'$, $G1$, $P$, $C$, $A$ bands related to the optically active centers, in process of annealing. Conventional designations of PL peaks were selected on the analogy with paper [14], which also studied the PL of extended defects introduced by implantation of Ge into Si. The fact that the position of 0.89 eV ($G1'$) and 0.936 eV ($G1$) bands in the PL spectra agrees well with the PL of {113} defects arising upon implantation of most different ions [23,24], confirms its independence on the impurity. This means that the decisice factor is transformation of the structure of the {113} defects in process of annealing. However, the widest $G2$ band in the region of $\sim 0.8$ eV arising after low temperature annealing $600-700\,^{\circ}$C, usually observed in PL spectra in Si upon implantation and annealing at $T > 1000\,^{\circ}$C and related to dislocations [25], must be unambiguously related to Ge accumulation in the plane of the {001} defects. This is confirmed by the fact that together with the growth of annealing temperature to $700\,^{\circ}$C, the size of {001} defects increases ($\sim$ 10 times) and their domination in the implanted layers of silicon, which is accompanied by amplification of the $G2$ band intensity (Figure 4, *b*). The analysis of the geometric phase of HREM images of {001}

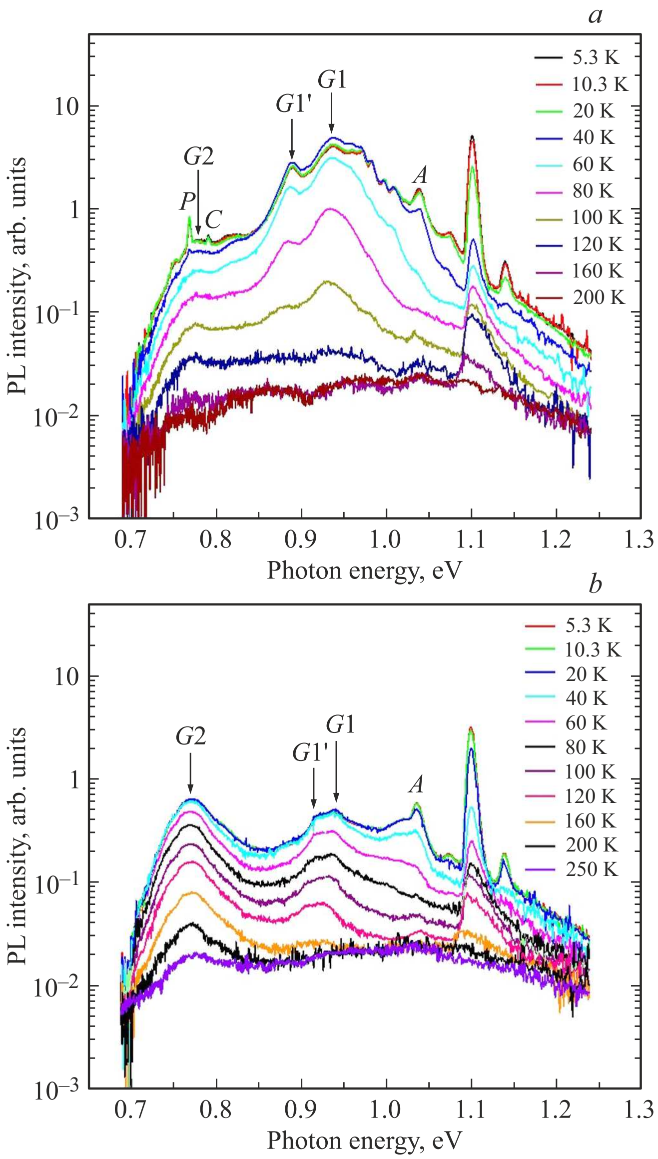


**Figure 4.** Temperature dependence of PL spectra of SOI structures radiated with $Ge^{+}$ ions and annealed at $600\,^{\circ}$C (*a*) and $700\,^{\circ}$C (*b*). The measurements were conducted in the temperature range from 5.3 to 250 K. The density of photoexcitation power of a laser with wavelength of 405 nm was 10 W/cm$^2$.

defects records the appearance of strong deformations related to Ge accumulation in their planes (Figure 3, *c*). The form of this accumulation is not yet clear and is possibly related to the initial localization of split Ge$-I_{\langle 110 \rangle}$ in the defect plane. Note that annealing at $800\,^{\circ}$C similarly to the implanted Si(001) wafer with $Ge^{+}$ ions is accompanied with the disappearance of $G1$, $G1'$ bands in the PL spectrum and the growth of $G2$ band intensity, related to the appearance of volume nanoinclusions of GeSi QDs (solid solution) [14], since the extended defects at $T > 700\,^{\circ}$C may not exist in virtue of their metastability [20]. At annealing temperatures $> 800\,^{\circ}$C all $G1$, $G1'$ and $G2$ bands disappear from PL spectra [14], which indicates diffuse dissolution of GeSi QD nanoinclusions.

After annealing at $T = 800\,^\circ$C in the PL spectra from SOI structures radiated with $Ge^+$ ions, $G1$, $G1'$ and $G2$ bands are not observed, which is fundamentlally different from the results of paper [14], where at this annealing temperature the signal $G2$ has maximum intensity. This makes it possible to assume that the true annealing temperature of SOI substrates used in our paper is $40-50\,^\circ$C higher than the temperature achieved at the heating of regular Si(100)-substrates. This agrees with the results of paper [26], which studied the features of SOI substrate heating under the conditions of molecular beam epitaxy.

Based on the processing of measured PL spectra, the temperature dependences were obtained between the integral PL intensity for the centers of radiative recombination of $G2$ type created with $Ge^+$ implantation into SOI substrates with subsequent thermal annealing, and the specific activation energies of PL suppression were defined. For the SOI structure annealed at $T = 600\,^\circ$C, the activation energy of PL suppression, when Ge nanoinclusions are observed in plane of $\{001\}$ defect, was $E_a \approx 52$ meV. Annealing of the SOI structure at $T = 700\,^\circ$C causes increase in the activation energy $E_a$ to 177 meV. However, the obtained value for $E_a$ was almost 2 times below the activation energy obtained for the PL suppression in Si(100) at annealing $800\,^\circ$C, when 10 nanometer inclusions of GeSi QDs are observed [14]. This makes it possible to assume that the annealing temperature $700\,^\circ$C is seemingly not sufficient to form the optimal shape of light-emitting centers in the SOI structure. Since already at $800\,^\circ$C in SOI structures the complete annealing of the defects generating signal $G2$ takes place, the optimal temperature of generation of optically active centers is likely to be near $750\,^\circ$C. More detailed studies are required for the conditions of generation of optically active defects in the structures developed on the basis of SOI substrates.

## 4. Conclusion

The optically active centers in SOI structures obtained using ion implantation of Ge and annealing in the temperature interval $600-700\,^\circ$C demonstrate approximately the same features in the PL spectra, as the centers developed on regular Si(100) substrates. However, the shape and structure of defects responsible for thermal stability of optically active centers differ noticeably. Quantitative deviation with the PL quenching activation energy values obtained in paper [14] depend on the difference under the conditions of formation of extended defects and nanoinclusions in the structures developed on the basis of SOI substrates.

### Funding

The study was conducted with the financial support of the Russian Scientific Foundation (grant No. 25-22-00424).

### Acknowledgments

The authors of the paper would like to express their gratitude to the State Program of Scientific Research „Material Science, New Materials and Technologies“, subprogram „Nanostructure“, for the luminescent measurements that were conducted within the assignment 2.2.1 (Belarus), and also to R.I. Batalov and V.F. Valeev from the Kazan Physical-Technical Institute, Federal Research Center, Kazan Scientific Center of the Russian Academy of Sciences for the implantation of germanium ions into silicon, „Nanostructures“ Common Use Center of the Institute of Semiconductor Physics, Siberian Branch of the Russian Academy of Sciences and „High Technologies and Analytics of Nanosystems“ Common Use Center of the Novosibirsk State University for making it possible to use technological and measurement equipment.

### Conflict of interest

Authors declare no conflict of interest.

## References

[1] M. Schatzl, F. Hackl, M. Glaser, P. Rauter, M. Brehm, L. Spindlberger, A. Simbula, M. Galli, T. Fromherz, F. Schäffler. ACS Photonics, **4**, 665 (2017). DOI: 10.1021/acsphotonics.6b01045

[2] L. Zhu, S. Yuan, C. Zeng, J. Xia. Adv. Opt. Mater., **8**, 1901830 (2020). DOI: 10.1002/adom.201901830

[3] L. Ding, Y.F. Yu, D. Morits, M. Yu, T.Y.L. Ang, H.-S. Chu, S.T. Lim, C.E. Png, R. Paniagua-Dominguez, A.I. Kuznetsov. Nanoscale, **12**, 21713 (2020). DOI: 10.1039/D0NR05248E

[4] Y. De Koninck, C. Caer, D. Yudistira, M. Baryshnikova, H. Sar, P.-Y. Hsieh, C.I. Özdemir, S.K. Patra, N. Kuznetsova, D. Colucci, A. Milenin, A.A. Yimam, G. Morthier, D.V. Thoūrhout, P. Verheyen, M. Pantouvaki, B. Kunert, J.V. Campenhout. Nature, **637**, 63 (2025). DOI: 10.1038/s41586-024-08364-2

[5] K. Eberl, M.O. Lipinski, Y.M. Manz, W. Winter, N.Y. Jin-Phillipp, O.G. Schmidt. Physica E, **9**, 164 (2001). DOI: 10.1016/S1386-9477(00)00190-9

[6] L. Tsybeskov, D.J. Lockwood. Proc. IEEE Optical Interconnects, **97**, 1284 (2009). DOI: 10.1109/JPROC.2009.2020711

[7] M. Brehm, M. Grydlik. Nanotechnology, **28**, 392001 (2017). DOI: 10.1088/1361-6528/aa8143

[8] L. Spindlberger, J. Aberl, L. Vukušić, T. Fromherz, J.-M. Hartmann, F. Fournel, S. Prucnal, F. Murphy-Armando, M. Brehm. Mater. Sci. Semicond. Process., **181**, 108616 (2024). DOI: 10.1016/j.mssp.2024.108616

[9] M. Grydlik, F. Hackl, H. Groiss, M. Glaser, A. Halilovic, T. Fromherz, W. Jantsch, F. Schaäffler, M. Brehm. ACS Photonics, **3**, 298 (2016). DOI: 10.1021/acsphotonics.5b00671

[10] M. Grydlik, M.T. Lusk, F. Hackl, A. Polimeni, T. Fromherz, W. Jantsch, F. Schäffler, M. Brehm. Nano Lett., **16** (11), 6802 (2016). DOI: 10.1021/acs.nanolett.6b02494

[11] F. Murphy-Armando, M. Brehm, P. Steindl, M.T. Lusk, T. Fromherz, K. Schwarz, P. Blaha. Phys. Rev. B, **103**, 085310 (2021). DOI: 10.1103/PhysRevB.103.085310
[12] L. Spindlberger, J. Aberl, A. Polimeni, J. Schuster, J. Hörschläger, T. Truglas, H. Groiss, F. Schäffler, T. Fromherz, M. Brehm. Crystals, **10**, 351 (2020). DOI: 10.3390/cryst10050351
[13] Zh.V. Smagina, V.A. Zinoviev, A.V. Mudry, O.M. Borodavchenko, A.O. Bazhenov, A.V. Dvurechensky, V.D. Zhivulko. FTP, **59** (2), 55 (2025) (in Russian).
[14] V.A. Zinovyev, A.F. Zinovieva, Zh.V. Smagina, A.V. Dvurechenskii, A.K. Gutakovskii, L.I. Fedina, O.M. Borodavchenko, V.D. Zhivulko, A.V. Mudryi. J. Appl. Phys., **130**, 153101 (2021). DOI: 10.1063/5.0063592
[15] R.I. Batalov, R.M. Bayazitov, V.I. Nuzhdin, P.I. Gayduk, S.L. Prokopiev, G.D. Ivlev. Izv. vuzov. Fizika, **54** (1-2), 59 (2011) (in Russian).
[16] J.J. Hamilton, N.E.B. Cowern, J.A. Sharp, K.J. Kirkby, E.J.H. Collart, B. Colombeau, M. Bersani, D. Giubertoni, A. Parisini. Appl. Phys. Lett., **89**, 042111 (2006). DOI: 10.1063/1.2240257
[17] V.A. Zinoviev, Zh.V. Smagina, S.A. Rudin, A.F. Zinovieva, A.V. Nenashev, E.E. Rodyakina, S.A. Dyakov, I.A. Smagin, M.V. Stepikhova, A.V. Novikov. FTP, **59**, 614 (2025) (in Russian). DOI: 10.61011/FTP.2025.02.60977.7726
[18] A.N. Mikhaylov, A.I. Belov, D.S. Korolev, A.O. Timofeeva, V.K. Vasiliev, A.N. Shushunov, A.I. Bobrov, D.A. Pavlov, D.I. Tetelbaum, E.I. Shek. FTP, **48**, 212 (2014) (in Russian).
[19] Zh.V. Smagina, N.P. Stepina, V.A. Zinovyev, P.L. Novikov, P.A. Kuchinskaya, A.V. Dvurechenskii. Appl. Phys. Lett., **105**, 153106 (2014). DOI: 10.1063/1.4898579
[20] A.L. Aseev, L.I. Fedina, D. Hoehl, H. Barsch. *Clusters of Interstitial Atoms in Silicon and Germanium* (Berlin: Academy Verlag, 1994).
[21] L.I. Fedina, A.K. Gutakovskii, A.V. Latyshev, A.L. Aseev. In: *Advances in Semiconductor Nanostructures, Growth, Characterization, Properties and Applications*, ed. by A.V. Latyshev, A.V. Dvurechenskii, A.L. Aseev (Elsevier, Amsterdam, 2017) p. 383.
[22] L.I. Fedina, S.A. Song, A.L. Chuvilin, A.K. Gutakovskii, A.V. Latyshev. Microsc. Microanal., **19** (S5), 38 (2013). DOI: 10.1017/S1431927613012294
[23] S. Coffa, S. Libertino, C. Spinella. Appl. Phys. Lett., **76**, 321 (2000). DOI: 10.1063/1.125733
[24] N.A. Sobolev, A.E. Kalyadin, E.I. Shek, K.F. Shtel'makh, V.I. Vdovin, A.K. Gutakovskii, L.I. Fedina. Phys. Status Solidi A, **214**, 1700317 (2017). DOI: 10.1002/pssa.201700317
[25] L.I. Fedina, A.K. Gutakovskii, T.S. Shamirzaev. J. Appl. Phys., **124**, 053106 (2018). DOI: 10.1063/1.5011329
[26] P.V. Volkov, A.V. Goryunov, D.N. Lobanov, A.Yu. Luk'yanov, A.V. Novikov, A.D. Tertyshnik, M.V. Shaleev, D.V. Yurasov. J. Cryst. Growth, **448**, 89 (2016). DOI: 10.1016/j.jcrysgro.2016.05.029

*Translated by M.Verenikina*